Frustration and slow dynamics of granular packings

Mario Nicodemi,[1,2] Antonio Coniglio,[1,2] and Hans J. Herrmann[1,3]
[1]*PMMH ESPCI, 10 rue Vauquelin, 75231 Paris Cedex 05, France*
[2]*Dipartimento di Scienze Fisiche, Universitá di Napoli ''Federico II,'' INFM and INFN, Sezione di Napoli, Mostra d'Oltremare, Pad. 19, 80125, Napoli, Italy*
[3]*ICA 1, Universität Stuttgart, Pfaffenwaldring 27, 70569 Stuttgart, Germany*
(Received 4 November 1996)

Density relaxation in a frustrated lattice gas subject to gravity and vibrations is explored via Monte Carlo simulations. A comparison to some recent experimental results on compaction of granular media gives good agreement, and interesting predictions are possible. [S1063-651X(97)15803-2]

PACS number(s): 05.45.+b, 46.10.+z, 81.20.Ev, 81.05.Rm

I. INTRODUCTION

Dynamical processes in granular media show fascinating behavior [1–4]. The particular role of disorder and fluctuations in granular dynamics has led several authors [1,5–7] to propose an analogy to frustrated statistical systems such as spin glasses [8].

Recently a frustrated lattice gas model has been introduced to describe static and dynamic properties of granular materials [9]. This microscopic model is based on an analogy with frustrated percolation [10], expressed in terms of a Hamiltonian formalism in which disorder and frustration are key elements. In this statistical model, ''vibrations'' play the role of temperature in usual thermal systems [1,11–13]. Its quenched disorder and the consequent frustration try to describe the general physical mechanisms underlying the phenomenon of ''geometrical'' frustration known in granular media. The same model, without the gravitational contribution in the Hamiltonian, has been previously related to the physics of the glass transition in glass forming liquids [14].

Here we describe the combined effects of vibrations and gravity in this model, and compare them to experimental data. A well known experiment with granular systems is the compaction of sand. When a box filled with loose packed sand is shaken at low amplitude, density visibly increases [15]. If in addition, the density goes beyond a definite threshold, the mechanical properties of sand abruptly change and the granular structure cannot be sheared any longer without a volume increase. This phenomenon, very important in practical applications [16], was observed by Reynolds [17], and is referred to as the ''Reynolds'' or ''dilatancy'' transition. In the present model an analogy appears between the cooperativity effects underlying the Reynolds transition in granular media and the actual spin glass transition where a diverging length naturally exists [7,9].

This paper also analyzes the grain density relaxation in different dynamical situations, and relates our observations to corresponding phenomena in real experiments. We find that in the present model the logarithmic behavior, known from experimental measurements in sequences of taps [15], is recovered, and further predictions are possible. We observe a different dynamical behavior for grain deposition in a single vibration process, where stretched exponentials are found. The robustness to changes of these structural properties is also analyzed.

II. MODEL

The model we study here is described in [9], and we briefly summarize its essential characteristics. It consists of a system of particles diffusing on a square lattice whose bonds are characterized by fixed random numbers $\epsilon_{ij}=\pm 1$ (see Fig. 1). On site i we set $n_i=1$ if a particle is present and 0 otherwise. Particles are characterized by an internal degree of freedom $S_i=\pm 1$ and are subjected to the constraint that whenever two (i and j) are neighboring, their ''spin'' must satisfy the relation

$$\epsilon_{ij}S_iS_j=1, \tag{1}$$

i.e., they have to fit the local ''geometrical'' structure. At high enough density, particles feel the effects of the ''quenched'' frustration imposed by the choice of the ϵ_{ij}. In fact, in resemblance to frustrated percolation [10], they can never close a frustrated loop in the lattice because along such loops the quantity $\Sigma_{i,j\in\text{loop}}(\epsilon_{ij}S_iS_j-1)$ cannot be zero [8] as imposed by the condition of Eq. (1). In the system there will then unavoidably be empty sites. The bond variables ϵ_{ij} model the general effects of geometrical frustration in granular systems due to the shapes and arrangements of particles.

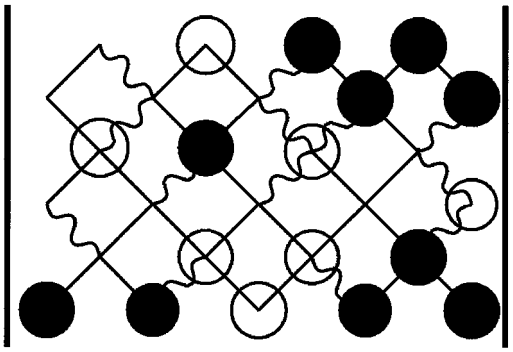

FIG. 1. Schematic picture of the lattice model considered here. Wavy and straight lines represent the two different kinds of bonds ($\epsilon_{ij}=\pm 1$). Filled (empty) circles are present particles with spin $S_i=+1$ ($S_i=-1$).

The internal variables S_i describe local quantities, as rotations and positions, which actually determine the geometrical frustration [6,7].

We want to study this system in presence of ''external vibrations'' and ''gravity.'' So we define a dynamics in our model as a random diffusion of particles on a square lattice tilted by 45° (see Fig. 1) in such a way as to preserve the constraints of Eq. (1). The particles attempt a move upward with probability P_2 and downward with P_1 (with $P_1+P_2=1$). The move is made only if the internal degrees of freedom satisfy Eq. (1). Similarly a spin flips with probability one if there is no violation of Eq. (1), and does not flip otherwise. In the absence of vibrations, the effect of gravity imposes $P_2=0$. When vibrations are switched on, P_2 becomes finite. The crucial parameter which controls the dynamics and the final density is the ratio $x(t)=P_2(t)/P_1(t)$ which describes the amplitude of the vibration.

This model can be described in terms of the following Hamiltonian in the limit $J\to\infty$ (see [9])

$$-H=\sum_{\langle ij\rangle} J(\epsilon_{ij}S_iS_j-1)n_in_j+\mu\sum_i n_i, \qquad (2)$$

where $S_i=\pm1$ are spin variables, $n_i=0$ and 1 occupancy variables, and $\epsilon_{ij}=\pm1$ quenched interactions associated with the bonds of the lattice. Hamiltonian (2) opens the way to a definite correspondence with disordered magnetic systems as spin glasses, and was actually proven to undergo a spin glass transition at high density (or low temperature) [14,18]. Here we just note that it reduces in the $\mu\to\infty$ limit to the usual $\pm J$ *Ising spin glass* [8], and in the limit $J\to\infty$ to a version of *site frustrated percolation* [10,14]. When the particle number is fixed, the configuration space of the system obtained in this last limit is the same as that of the frustrated lattice gas introduced at the beginning of this section.

The Monte Carlo simulations of the model described above are performed on a tilted lattice with periodic boundary conditions along the x axis and rigid walls at bottom and top. After fixing the random quenched ϵ_{ij} on the bonds, a random initial particle configuration is prepared by randomly inserting particles of given spin into the box from its top and then letting them fall down, with the described dynamics ($P_2=0$), until the box is filled. The two basic Monte Carlo moves (the spin flip and particle hopping) are done in random order. To obtain an initial low density configuration we do not allow particle spins to flip in this preparation process. The state prepared in this way has a density of about 0.518 which corresponds to a random loose packing particle in two dimensions.

III. SIMULATING VIBRATIONS

As already mentioned, we study the effects of ''vibration'' by using a finite value for P_2. It is experimentally known that sand, randomly poured into a box, reaches higher density states after shaking. Let us explore this phenomenon in our model.

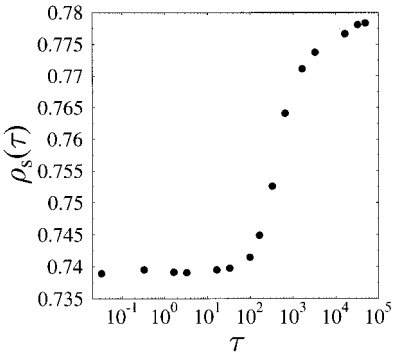

FIG. 2. Final bulk density $\rho_s(\tau)$, in static configurations, as a function of the logarithm duration τ of the vibration, for a box of size 100×200. A characteristic vibration duration $\tau^*\approx2\times10^2$ appears, below which the final density ρ_s is not affected by the vibrations.

A. Density relaxation in a single ''tap''

As first we choose to decrease the initial ratio $x_0=P_2(t=0)/P_1(t=0)$ in time according a linear law as $x(t)=x_0(1-t/\tau)\theta(\tau-t)$ and $t>0$, where τ is the duration of the vibration or the inverse velocity of quenching (we take $x_0=1$). This process corresponds, in the magnetic analogy, to a quench of the system from a high temperature state. With this procedure the systems attains a final ''static'' configuration which is defined by the criterion that during a fixed time $t_{\rm repose}$ nothing changes any longer. In our simulation we fixed $t_{\rm repose}=330$ much longer than any intrinsic time in absence of vibration. Time t is measured in such a way that one unit corresponds to one single average update of all particles and all spins of the lattice.

The data we present in this section were obtained in a box of size 100×200, and their states have been averaged over 32–512 different $\{\epsilon_{ij}\}$ configurations (according to the value of τ). These values, as those used below, are chosen to control finite size effects on our Monte Carlo data as much as possible. They are large enough to say that our results are strongly robust to size changes.

After a vibration cycle has been applied as described above, the system presents final densities which clearly depend on the value of the τ of the vibrations. As depicted in Fig. 2, the final ''static'' bulk density $\rho_s(\tau)$, defined as the mean density in the lower 25% of the box, increases asymptotically with τ, reaching an ideal maximal density value ρ_m when $\tau\to\infty$ (from our data we have roughly $\rho_m\approx0.79$). From the data in Fig. 2 one sees that a characteristic value of τ exists, below which vibrations do not affect the final ρ_s. For our system size this value τ^* corresponds to about $\tau^*\approx2\times10^2$.

During the dynamical process described above, we have recorded the time dependence of the mean bulk density $\rho(t,\tau)$, measured as the mean density in the lower 25% of the box at time t as depicted in Fig. 3. At $t=0$ the density starts from the initial low value defined by our preparation rule $\rho_i=0.518$. With increasing time, it approaches a definite plateau which corresponds to the ''static'' limit $\rho_s(\tau)$. It is evident that this process takes places on time scales which depend drastically on τ. In contrast to the functional form proposed by other models (see, for instance, those quoted in

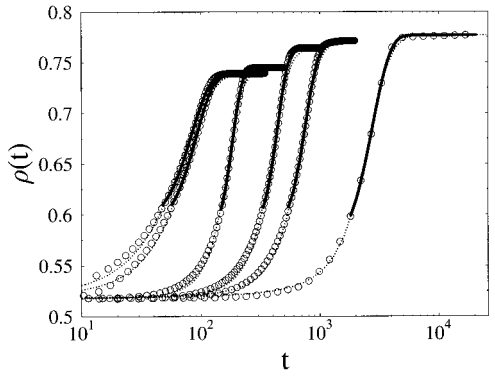

FIG. 3. Bulk density $\rho(t,\tau)$ relaxation, in a single vibration process (a single ''tap''), as a function of log time t for different values of the vibration duration τ (from left to right $\tau=1.64\times10^0$, 1.64×10^1, 1.64×10^2, 6.56×10^2, 1.64×10^3, and 1.64×10^4). The density starts from a definite value $\rho_i=0.518$, which depends on the preparation process of the initial configuration, and grows to the final value $\rho_s(\tau)$ reported in Fig. 2. Dashed lines are fits using Eq. (3), and bold continuous lines are stretched exponential fits according to Eq. (5), as explained in the text. Their parameters are respectively reported in Figs. 4 and 6.

[19–21]), our data are reasonably well fitted by a Fermi-Dirac function

$$\rho(t,\tau)=\rho_s(\tau)-[\rho_s(\tau)-\rho_i](1+e^{-t_0/\tau_0})/[1+\exp((t-t_0)/\tau_0)], \quad (3)$$

where $\rho_s(\tau)=\lim_{t\to\infty}\rho(t,\tau)$. These fits are shown by the dashed line in Fig. 3 ($\rho_i=0.518$ is the initial state density). The two fitting parameters τ_0 and t_0 are reported in Fig. 4. They undergo a change of behavior at $\tau\sim\tau^*$:

$$\tau_0(\tau)=\tau_<,\quad t_0(\tau)=\tau/t_1+t_< \quad \text{if } \tau<\tau^*,$$

$$\tau_0(\tau)=(\tau/\tau_2)^\alpha+a, t_0(\tau)=(\tau/t_2)^\alpha+b \quad \text{if } \tau>\tau^*, \quad (4)$$

where $\tau_<=26$, $\tau_2=0.5$, $t_<=48$, $t_1=1.15$, $t_2=0.02$, and $\alpha=0.6$ ($a=-12$ and $b=-5$). τ^* is actually defined as the intersection point of the two curves in Eq. (4). The data for the density relaxation may be rescaled according to Eq. (3), and the scaling plot is given in Fig. 5. This picture reveals that, although the data scale well with respect to the variable $(t-t_0)/\tau_0$, for long times the simple master function provided by Eq. (3), which implies an exponential relaxation, seems to show a small but systematic deviation from the Monte Carlo (MC) data. These observations lead us to try better fits in this long time region and our data seem well fitted by a ''stretched exponential'' form

$$\rho(t,\tau)=\rho_s(\tau)-f[\rho_s(\tau)-d_0]\exp[-((t-t_0)/\tau_0)^\beta], \quad (5)$$

as shown in Fig. 3 with the bold continuous lines. In Eq. (5) d_0 is an initial arbitrary density (we take $d_0=0.60$) above which we actually make the fit. This is a four parameter fit; however, we find that one can take the factor f equal to $f=1.3$ and the exponent $\beta=2.3$ as independent of τ. The parameters τ_0 and t_0 of Eq. (5) have moreover nearly the same behavior as a function of τ as the ones described above for the parameters of Eq. (3) (see Fig. 6). Also in this case Eq. (4) approximately holds [actually $\tau_<=62$, $\tau_2=0.2$, $a=-19$, and $\alpha=0.67$ for $\tau_0(\tau)$, and $t_<=25$, $t_1=1.6$, $t_2=0.0008$, $b=-56$, and $\alpha=0.42$ for $t_0(\tau)$]. The relaxation

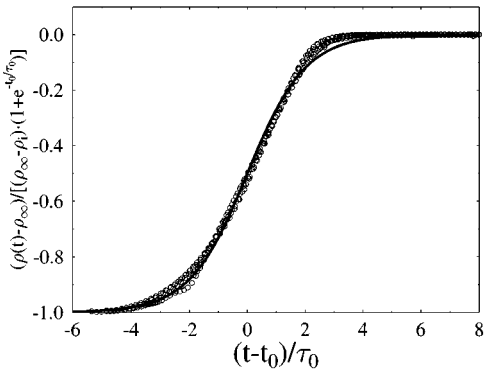

FIG. 5. Bulk density $\rho(t,\tau)$ relaxation, in a single vibration process, given in Fig. 3, rescaled according to Eq. (3), which is the continuous line in this picture, as a function of rescaled time $(t-t_0)/\tau_0$.

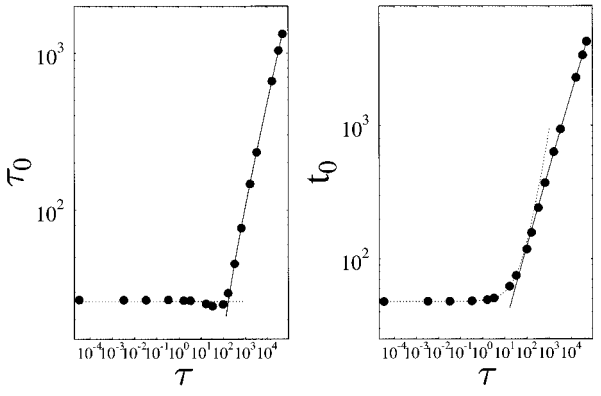

FIG. 4. Parameters τ_0 and t_0 of fits from Eq. (3) for the density relaxation after a single ''tap'' depicted in Fig. 3, as a function of the logarithm of the vibration duration τ. Their (power law) behavior abruptly changes at τ^*, the characteristic vibration duration below which the final ρ_s is not affected. The two superimposed curves are fits described in Eq. (4).

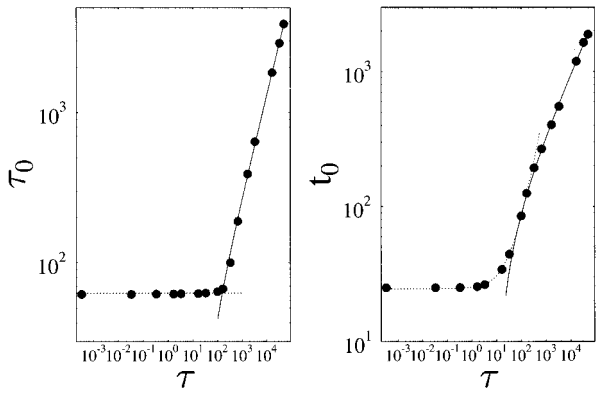

FIG. 6. Parameters of the stretched exponential fit, τ_0 and t_0 [see Eq. (5)], from the fit of density relaxation in the long time region of a single vibration process, as a function of the logarithm of the vibration duration τ. Their behavior is analogous to the one described in Fig. 4.

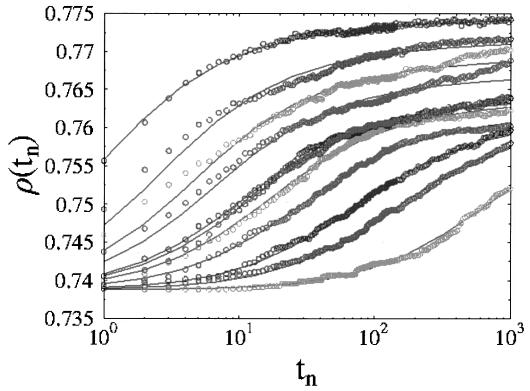

FIG. 7. Static bulk density $\rho(t_n)$ from our MC data as a function of tap number t_n, for tap vibrations of amplitude $x_0=1.0\times10^{-4}$, 5.0×10^{-4}, 1.0×10^{-3}, 2.0×10^{-3}, 5.0×10^{-3}, 7.0×10^{-3}, 1.0×10^{-2}, 2.0×10^{-2}, 5.0×10^{-2}, 0.1, 0.5 (from bottom to top), and duration $\tau=3.28\times10^1$. The continuous curves are logarithmic fits from Eq. (7), the parameters of which are given in Fig. 9.

process here explored corresponds experimentally to the density relaxation after a single application of vibrations to the box (a single ''tap'').

B. Sequences of taps

In connection to recent experiments on compaction dynamics in granular media, we also studied the phenomena of density relaxation during a sequence of taps. Experimentally a ''tap'' is the shaking of a container filled with grains by vibrations of given duration and amplitude. In the following MC simulations, each single tap is a process in which vibrations are applied, to our particle on the lattice, according to a law $x(t)=x_0=\text{const}$ for $t\in[0,\tau]$ and then the system is let to find a stationary state for a time t_{repose} in which $x(t)=0$. So here τ is the duration of the vibration. After each tap we measure the static bulk density of the system $\rho(t_n)$ (t_n is the nth tap number). We repeat the tapping sequence for different values of the tap amplitude x_0 and fixed duration τ (see Fig. 7). For this Monte Carlo experiment, which was very CPU-time consuming, we considered a system of size 30×60, averaged over 32 different ϵ_{ij} configurations, and fix $\tau=36.69$.

To describe experimental observations about grain density relaxation under a sequence of taps a logarithmic law was proposed in Ref. [15]:

$$\rho(t_n)=\rho_\infty-\Delta\rho_\infty/[1+B\ln(t_n/\tau_1+1)]. \tag{6}$$

This law has proved to be satisfied very well by relaxation data in the present model [9], which can be excellently rescaled with experimental data using this four parameter fit as shown in Fig. 8.

In addition our MC data allow us to give more insight into the parameters of Eq. (6). After a few manipulations, Eq. (6) may be transformed into

$$\rho(t_n)=\rho_\infty-\ln(c)(\rho_\infty-\rho_0)/\ln(t_n/\tau_0+c), \tag{7}$$

where $\ln(c)=1/B$, $\tau_0=\tau_1/c$, and we have written in explicit form the asymptotic variation in density as the difference of a final asymptotic value (ρ_∞) and an initial value (ρ_0), i.e., $\Delta\rho_\infty=\rho_\infty-\rho_0$.

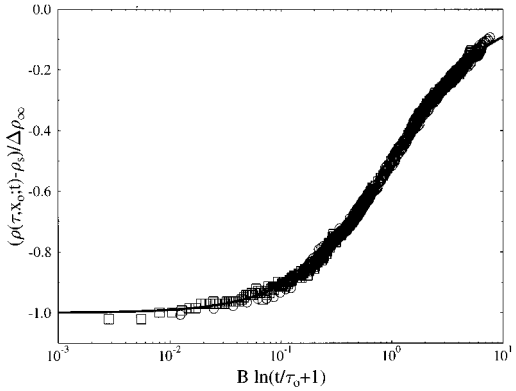

FIG. 8. Experimental data from Knight *et al.* (square) and our MC data (circle) on density relaxation $\rho(t_n)$ in a sequence of taps, as a function of tapping number t_n, rescaled according to the logarithmic function given in Eq. (6).

We find that for a sequence of our MC taps of fixed duration τ and amplitude x_0, Eq. (7) is an excellent fit even fixing the parameter $c=1.3$ as independent of x_0 (we now work at fixed τ) and imposing that the fit function passes at $t_n=0$ in $\rho_0=0.7388$, i.e., the measured static initial state density of our system, obtained from the prepared random starting configuration letting the particles just go down and their spin flip according the given rules. In this way we can reduce to just two the parameters to optimize in the fits with Eq. (6). The phenomenological parameter c may be interpreted as the ratio of two typical times in the system ($c=\tau_1/\tau_0$), and the finding that it is constant with the vibration amplitude x_0 in the range explored $x_0\in[1.0\ \ 10^{-4},0.5]$ suggests that in our model these are proportional to each other.

Our results for the density relaxation are shown in Fig. 7, and the values of the two fitting parameters ρ_∞ and τ_0 in Fig. 9. The parameter τ_0, at fixed $\tau=36.69$, seems to be a simple power law of the vibration amplitude x_0:

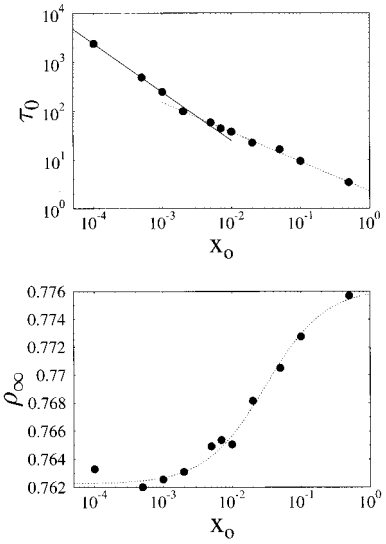

FIG. 9. Fit parameters ρ_∞ and τ_0 for density relaxation from Eq. (7), as a function of vibration amplitude x_0. $\tau_0(x_0)$ seems to be well described by two simple power laws.

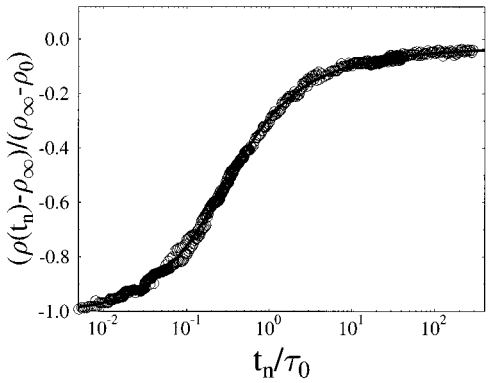

FIG. 10. Our MC data (circles) of the density relaxation in a sequence of taps of fixed amplitude and duration rescaled according to Eq. (7) with two parameters (given in Fig. 9), as a function of rescaled tap number t_n/τ_0. Equation (7) gives the muster curve $-\ln(c)/\ln(x+c)$ with $c=1.3$, drawn as a continuous line.

$$\tau_0(x_0)=(x_0/X)^{-\gamma}. \tag{8}$$

For low x_0 the exponents are $\gamma=1$ and $X=0.26$, but data show a crossover to $\gamma=0.6$ and $X=3.9$ above $x_0^*\approx 4\times 10^{-3}$. The law which links ρ_∞ to x_0 appears to be less simple. A possible fit for intermediate values of x_0 is

$$\rho_\infty(x_0)=r-1/(x_0/X_1+K), \tag{9}$$

with $r=0.776$, $K=70$, and $X_1=4\times 10^{-4}$. To show the quality of the fit, our Monte Carlo data corresponding to 11 different time series in a range of four orders of magnitude in the vibration amplitude x_0 ($x_0\in[1.0\ 10^{-4},0.5]$), rescaled according to Eq. (7) with these given two parameters values, are presented in Fig. 10.

As stated above and proved in [15], Eq. (7) gives a good four parameter fit for experimental data about density relaxation in a tapping sequence. Interestingly we find, moreover, that it is possible to produce a good quality fit for these data also with the parameter c considered as a constant. Our previous analysis, based on four experimental time series from Knight *et al.* [15] (their lower capacitor measurements), shows that c is bounded in a short interval. The average over the previous values of c of the four series gives $c=1.4$, and with this fixed parameter we produced a good fit of data from Ref. [15]. The fit is shown in Fig. 11 for these experimental data, and its three parameters depicted in Fig. 12. For the two intermediate vibration amplitude series it is also possible to produce excellent fits with just two parameters, fixing ρ_0 to the actual experimentally measured initial configuration density. A fit of experimental data with $c=1.3$ is just slightly poorer. It would be interesting to analyze other experimental data after the insight of these theoretical results, and to produce measurements to better understand the limits of the presented model and test its main forecasts.

It is a well known fact, in granular media, that the properties of the system in a given configuration strongly depend on its preparation and past history. Specifically, if you make a transformation, closing a loop in the parameters space of the system, the final state strongly depends on the details of the path and not just on the final values of the parameters. Previous data show that this occurs in this lattice model too.

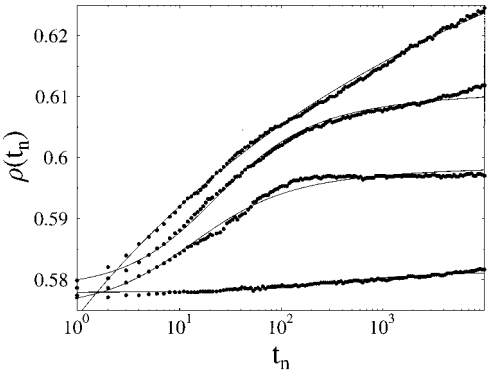

FIG. 11. Experimental data from Knight *et al.* on grain density relaxation $\rho(t_n)$ in a sequence of taps for four different values of vibrations amplitude, as a function of the tap sequence number t_n. The continuous superimposed lines are fits according to Eq. (7), fixing the parameter c to a constant value $c=1.4$. The parameters of the fit are reported in Fig. 12.

We performed also another Monte Carlo experiment with our frustrated lattice gas model, which concerns short sequences of taps in which the vibration amplitude x_0 is varied at fixed amplitude increment Δx_0 holding constant their duration τ. The process actually consists in a sequence of $2m-1$ taps, of amplitude $x_1\cdots x_n\cdots x_{2m-1}$, from an initial amplitude $x_i=0=x_1$ to a maximal amplitude $x_f=0.6=x_m$ and then back again to $x_i=0=x_{2m-1}$: more precisely, the sequence of amplitudes is $x_n=x_i+(n-1)\Delta x_0$ if $n\leqslant m$ and $x_n=x_f-(n-m)\Delta x_0$ if $n>m$ (see Fig. 13). This analysis allows us, moreover, to test the validity of our previous findings about the universality of the relaxation processes described by Eq. (7).

Our data for the system described above of size 30×60, averaged over 32 different ϵ_{ij} configurations, are depicted in Fig. 14 for three different values of τ ($\tau=3.67\times 10^0$, 3.67×10^1, and 3.67×10^2) and four different values of Δx_0 ($\Delta x_0=0.025$, 0.05, 0.1, and 0.2). We find that these data may be described by a law formally equal to Eq. (7),

$$\rho(x)=\rho_\infty-\ln(c)(\rho_\infty-\rho_0)/\ln(x/\chi_0+c), \tag{10}$$

where the constant c is set again to $c=1.3$, the same value used before in Eq. (7). Here, in Eq. (10), the equivalent time variable x is chosen to be $x=x_n$ for the increasing ramp, and

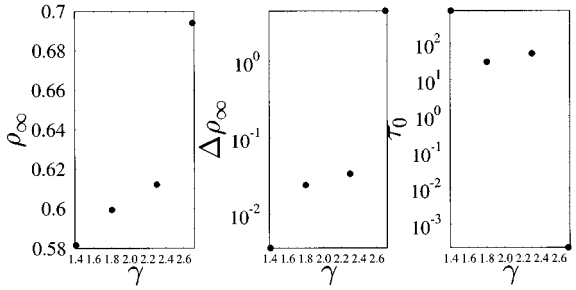

FIG. 12. Fit parameters from Eq. (7) for the experimental data of Knight *et al.* on grain density relaxation presented in Fig. 11. The parameters are reported as a function of γ ($\gamma=1.4$, 1.8, 2.3, and 2.7), the ratio of the peak acceleration of a tap, a, to $g=9.81$ m/s^2, the gravitational acceleration ($\gamma=a/g$).

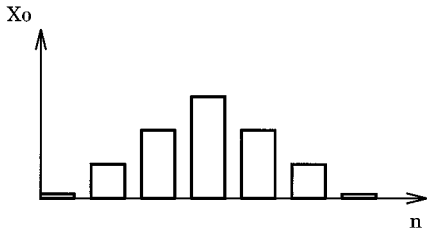

FIG. 13. This picture depicts the sequence of amplitude x_0 of the second kind of tapping sequence we study in the paper, as a function of the tapping number n. Here the amplitude is linearly increased and then decreased with fixed single ''tap'' duration τ and amplitude increment (or decrement) Δx_0.

to be $x=x_f-x_n$ for the decreasing ramp, respectively. The starting density value ρ_0 is set, as in Eq. (7), equal to $\rho_0=0.7388=\rho(x_i)$ to fit the increasing amplitude ramp of the sequences (lower wings of Fig. 14), and to $\rho(x_f)$ for the decreasing amplitude ramp (upper wings of Fig. 14).

The fits of our data with Eq. (10) are the superimposed continuous curves in Fig. 14, and the fitting parameters $\rho_\infty(\tau,\Delta x_0)$ and $\chi_0(\tau,\Delta x_0)$ are reported in Fig. 15. Our Monte Carlo data rescaled according Eq. (10) are reported in Fig. 16.

The characteristics of the present tapping sequence are very different from the others presented before, and so the good quality of this last scaling confirms the stability of the structure for the relaxation represented by Eq. (7). Moreover, the finding that in our model the constant c seems very robust to changes in the tapping process is surprising.

IV. DIFFUSIVITY PROPERTIES

To characterize the state of the packing and its capability for internal rearrangement, we studied particle self-diffusivity at fixed global density by setting $x=1$. Specifically it is possible to study the particle mean square displacement $R^2(t)=\langle(1/N)\Sigma_i(r_i(t)-r_i(0))^2\rangle$. A very interesting phenomenon is observed for densities close to the maximal value ρ_m: $R^2(t)$ shows deviations from the linear time dependence typical of standard Brownian diffusive motion and presents an inflection point as depicted in Fig. 17 for a system of size 32×32. This signals the existence of two characteristic time regimes for particle motion (as already argued in [19]).

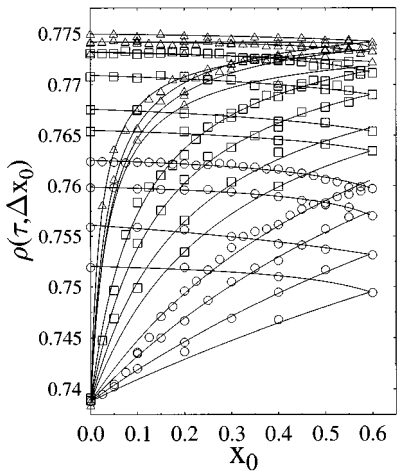

FIG. 14. Density relaxation for a sequence of taps where the amplitude is linearly increased (lower wings) and then decreased (upper wings), with fixed single ''tap'' duration τ and amplitude increment (or decrement) Δx_0. The data are taken for $\tau=3.67$ (circles), 3.67×10^1 (square), and 3.67×10^2 (triangles) and, at each fixed τ, for $\Delta x_0=0.025$, 0.05, 0.1, and 0.2 (from top to bottom of each series). Superimposed fits are from Eq. (10), and their parameters are depicted in Fig. 15.

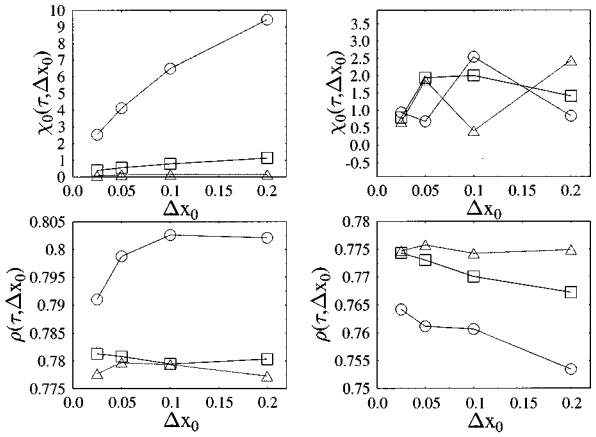

FIG. 15. Parameters of data fits, from Eq. (10), for the density relaxation described in Fig. 14. Left: ρ_∞ and χ_0 for data in lower wings of Fig. 14, with $\tau=3.67$ (circles), 3.67×10^1 (square), and 3.67×10^2 (triangles). Right: analogously for upper wings.

From the long time behavior of $R^2(t)\sim Dt$ we extract the diffusion coefficient $D(\rho)$, which goes to zero at about ρ_m, signaling a localization transition in which particles are confined in local cages and the macroscopic diffusionlike processes are suppressed (see Fig. 18). This phenomenon may also be described in a different way: ρ_m is the density above which it becomes impossible to obtain a macroscopic rearrangement of the particle positions without increasing the system volume, i.e., the density at which macroscopic shear in the system is impossible without dilatancy. This then seems to correspond to the quoted Reynolds transition in real granular media.

As shown above, two time regimes for particle motion

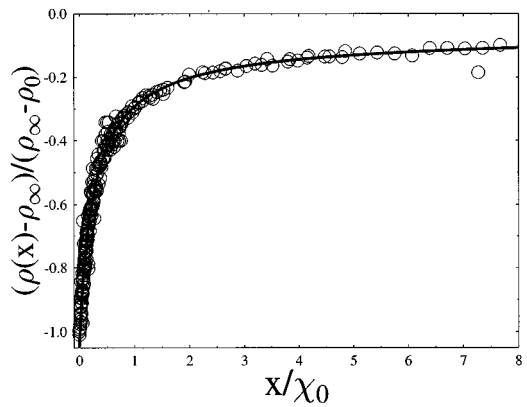

FIG. 16. Density relaxation data from Monte Carlo experiments described in Fig. 14, rescaled according to Eq. (10), with the parameters given in Fig. 15. The full line gives the analytic form of Eq. (10).

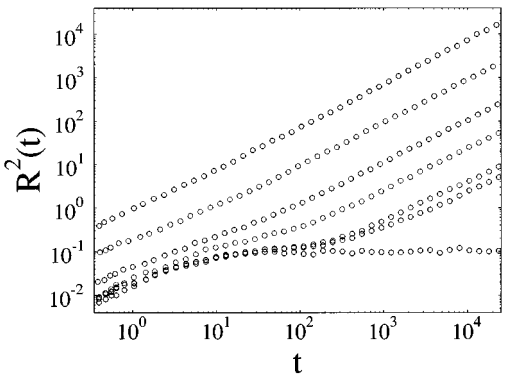

FIG. 17. Log-log plot of particle mean square displacement $R^2(t)$ as a function of time at different system densities. From above the fixed densities are $\rho_s = 0.3057$, 0.5771, 0.7412, 0.7734, 0.7814, 0.7823, and 0.7832. A sharp transition, at the maximum density, to a state with suppressed macroscopic diffusion is clearly visible.

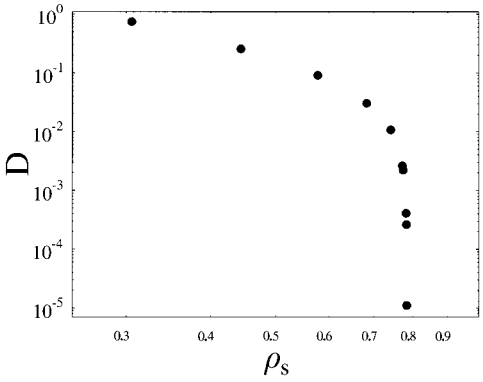

FIG. 18. Log-log plot of diffusivity constant $D(\rho)$ as a function of the density ρ_s. It decreases to zero at about $\rho_m \approx 0.79$.

appear in this model. This corresponds to the known fact that time correlation functions of Hamiltonian (2) have two characteristic times at high densities (low temperatures) [14]. The shorter is linked to the motion of particles inside cages of other particles, while the longer corresponds to macroscopic diffusionlike motion.

V. SPIN GLASS TRANSITION

The density ρ_m interestingly coincides with the density at which the spin glass (SG) transition of Hamiltonian (2) (for $J \to \infty$) is located. This would imply that at ρ_m the SG correlation length ξ_{SG} diverges, signaling the presence of collective behavior in the system. In SG this length is infinite in the whole region below the transition when it exists. Only some quantities, as ξ_{SG} or the nonlinear susceptibility $\chi_{\mathrm{SG}} = [(1/N)\Sigma_{ij} g_{ij}^2]_{\mathrm{av}}$, with $g_{ij} = \langle S_i n_i S_j n_j \rangle$, present clear divergences at the SG transition. On the contrary, quantities like the specific heat, the linear susceptibility, or the compressibility have no divergent critical behavior and look quite smooth around the critical point. In two dimensions (2D), the SG and the diffusivity transitions occur at the highest possible density in the system. In that sense the transition in 2D is only ''dynamical:'' one sees an effective transition the position of which slowly shifts to larger densities for longer observation times. We expect the same to occur in 2D for the Reynolds transition too. The coincidence of the SG transition and the suppression of self-diffusivity suggest a correspondence between the Reynolds transition in granular media, the SG transition in magnetic systems, and the ''ideal'' glass transition in glass-forming systems [7,14].

VI. CONCLUSIONS

We have studied a frustrated lattice gas linked to a spin glass and to frustrated percolation, which gives agreement with the dynamic behavior of granular media. It shows compaction and a typical logarithmic relaxation of density under tapping, as found in experiments [15]. It moreover naturally signals a correspondence between the Reynolds transition in granular media and the spin glass transition in magnetic alloys [7,9]. The same model has also been exploited to give microscopic insight into static stress distributions in disordered granular systems, where agreement was also found with experimental results [9]. Previously, without the gravitational term in its Hamiltonian, it has been related to the physics of the glass transition in glass forming liquids [14].

A common aspect, from the microscopic point of view, which appears in all these seemingly different materials is the existence of mechanisms leading to frustrations, as quenched disorder of the spin interactions in spin glasses, steric constraints, and the subsequent grain interlocking in granular media or the formation of local arrangements of molecules which kinetically prevent all the molecules from reaching the crystalline state in glass-forming liquids. From the thermodynamic point of view, the model studied here clarifies the analogy between the role that vibrations play in non-thermal systems as granular media and role of temperature in thermal systems as spin glasses or glass-forming liquids.

ACKNOWLEDGMENT

We thank IDRIS for computer time on Cray-T3D, and M.N. the ''Universitá di Napoli Federico II'' for financial support.

[1] H. M. Jaeger and S. R. Nagel, Science **255**, 1523 (1992); H. M. Jaeger, S. R. Nagel, and R. P. Behringer, Phys. Today **49**, 32 (1996).

[2] *Disorder and Granular Media*, edited by D. Bideau and A. Hansen (North-Holland, Amsterdam, 1993).

[3] *Granular Matter: an Interdisciplinary Approach*, edited by A. Mehta (Springer-Verlag, New York, 1994).

[4] C.-h. Liu, S. R. Nagel, D. A. Schecter, S. N. Coppersmith, S. Majumdar, O. Narayan, and T. A. Witten, Science **269**, 513 (1995).

[5] J. Souletie, J. Phys. (Paris) **44**, 1095 (1983).
[6] P. Evesque and D. Sornette, J. Mech. Behav. Mater. **5**, 261 (1994); A. Sornette, D. Sornette, and P. Evesque, Nonlinear Proc. Geophys. **1**, 209 (1994).
[7] A. Coniglio and H. J. Herrmann, Physica A **225**, 1 (1996).
[8] For a recent review, see K. Binder and P. Young, Adv. Phys. **41**, 547 (1992).
[9] M. Nicodemi, A. Coniglio, and H. J. Herrmann (unpublished).
[10] A. Coniglio, Nuovo Cimento **16D**, 1027 (1994); in *Correlation and Connectivity*, edited by H. E. Stanley and N. Ostrowsky (Kluwer, Dordrecht, 1990); A. Coniglio, F. di Liberto, G. Monroy and F. Perrugi, Phys. Rev. B **44**, 12 605 (1991).
[11] H. M. Jaeger, Chu-heng Liu, and S. R. Nagel, Phys. Rev. Lett. **62**, 40 (1988).
[12] S. Ogawa, in *Proceedings of the U.S.-Japan Symposium on Continuum Mechanics and Statistical Approaches to the Mechanics of Granular Media*, edited by S. Cowin and M. Satake (Gakujutsu Bunken, Fukyu-kai, 1978), p. 208.
[13] H. J. Herrmann, J. Phys. II **3**, 427 (1993).
[14] M. Nicodemi and A. Coniglio (unpublished).
[15] J. B. Knight, C. G. Fandrich, C. Ning Lau, H. M. Jaeger, and S. R. Nagel, Phys. Rev. E **51**, 3957 (1995).
[16] Y. M. Bashir and J. D. Goddard, J. Rheol. **35**, 849 (1991); P. A. Vermeer and X. de Borst, Heron **29**, 1 (1984).
[17] O. Reynolds, Philos. Mag. **20**, 469 (1885).
[18] J. Arenzon, M. Nicodemi, and M. Sellitto, J. Phys. (France) I **6**, 1 (1996).
[19] T. A. J. Duke, G. C. Barker and A. Mehta, Europhys. Lett. **13**, 19 (1990).
[20] E. Ben-Naim, J. B. Knight, and E. R. Nowak (unpublished).
[21] D. C. Hong, S. Yue, J. Rudra, M. Choi, and Y. Kim, Mod. Phys. Lett. B **6**, 761 (1992).